

## Cosmic-Ray Production Rate and Mean Removal Time of Beryllium-7 from the Atmosphere

PAUL A. BENIOFF\*

Tracerlab, Incorporated, Western Division, Richmond, California

(Received May 25, 1956)

The Be<sup>7</sup> production rate is given by the product of the nucleon flux ( $E_{\text{nucleon}} \geq 40$  Mev), the Be<sup>7</sup> production cross section, and an appropriate constant. The nucleon flux (as a function of altitude and latitude) is determined for  $E_{\text{nucleon}} \geq 500$  Mev from the fairly complete theoretical treatment available in the literature. For nucleons with energy between 40 Mev and 500 Mev, an approximate theory given in the literature is used. The sum of these two gives the nucleon flux applicable to Be<sup>7</sup> production. The Be<sup>7</sup> production cross section is obtained by multiplying the  $C(p, X)\text{Be}^7$  excitation function available in the literature by the  $N(p, X)\text{Be}^7/C(p, X)\text{Be}^7$  ratio obtained at Bev energies.

The Be<sup>7</sup> production rate in the atmosphere as a function of latitude and altitude is then obtained. Since the main errors lie in the determination of the nucleon flux, the derived flux curves are compared to literature data on the latitude effect and star

production rate. The agreement is found to be satisfactory and error limits are placed at  $\pm 50\%$ .

The mixing and washout processes in the atmosphere are then considered. The production rate of Be<sup>7</sup> in the stratosphere is found to be 5.0 atoms/cm<sup>2</sup> min, and 1.3 atoms/cm<sup>2</sup> min for the troposphere (assumed tropopause = 35 000 ft). The production rates are used with the rain water removal rate to determine the stratosphere mean removal time as a function of the troposphere mean removal time. Curves of this function are presented for three different average tropopause elevations (30 500 ft, 35 000 ft, 40 000 ft). Compared to these curves, the approximate literature values of 120 days and 14 days for Be<sup>7</sup> mean removal times from the stratosphere and troposphere respectively, seem too short. Longer times are indicated, of the order of years for the stratosphere, and three weeks or more for the troposphere. Recent experimental evidence in the literature appears to confirm this.

### INTRODUCTION

IT has been known for some time that cosmic rays produce many different isotopes by nuclear interactions with the gas nuclei of the atmosphere. Experimental evidence for the atmospheric production of tritium<sup>1</sup> and carbon-14<sup>2</sup> has existed for several years and more recently Be<sup>7</sup> has also been found.<sup>3</sup> The small amount of argon present in the atmosphere would account for the recently observed P<sup>32</sup> and Cl<sup>36</sup> in rain water.<sup>4,5</sup> Much information, about both cosmic rays and the atmosphere, can be learned if the amounts of various isotopes produced as a function of latitude and altitude are known. Be<sup>7</sup> is an interesting isotope to study both theoretically and experimentally because of its convenient half-life and sufficiently detectable radiation.

The theoretical development of the nucleon flux for the medium-energy range ( $E_{\text{nucleon}} < 500$  Mev) is not advanced enough to warrant use of an exact method of determining the Be<sup>7</sup> production rate as a function of altitude and latitude. Consequently, in this report, several simplifying approximations are used.

### NUCLEON FLUX ( $E \geq 500$ MEV)

By application of diffusion equations to the nucleon cascade occurring in the atmosphere, Messel<sup>6</sup> has cal-

culated the relative numbers of neutrons and protons with energy  $\geq 500$  Mev incident in the vertical direction as a function of altitude and geomagnetic latitude. (The meson contribution to Be<sup>7</sup> production can be neglected.) To convert these relative directional intensities into relative total intensities, the Gross transformation can be applied for vertical intensities at depths  $\geq 600$  g/cm<sup>2</sup> ( $\leq 14$  500 ft elevation) where absorption is nearly exponential. At depths less than 600 g/cm<sup>2</sup> the absorption deviates sufficiently from an exponential variation with atmospheric depth so that for accurate work a numerical integration must be used. The integral

$$I = 2\pi \int_0^{\pi/2} J(h/\cos\theta, E_c/E) \sin\theta d\theta$$

is evaluated numerically for a given vertical depth,  $h$ , and a given  $E_c/E$ , the ratio of the geomagnetic cut-off energy to the lower limit of the nucleon energy. The quantity  $J(h/\cos\theta, E_c/E)$  is read from the appropriate curve in Fig. 15 of reference 6, where, for a given zenith angle,  $\theta$ , the quantity  $h/\cos\theta$  is the atmospheric depth in the direction  $\theta$ . The slopes of the curves for depths  $\geq 600$  g/cm<sup>2</sup> are the same. Consequently the absorption mean free path may be considered constant with latitude, and equal to 125 g/cm<sup>2</sup>.<sup>8</sup> This value is used in the Gross transform.

To convert the relative total intensity to absolute intensity, the flux of primary nucleons at the top of the atmosphere at a given latitude must be known. The best value for the absolute primary vertical flux between 52° and 56° North geomagnetic latitude and zero

\* Present address: Department of Chemistry, Radiation Laboratory, University of California, Berkeley 4, California.

<sup>1</sup> S. Kaufman and W. Libby, *Phys. Rev.* **93**, 1337 (1954).

<sup>2</sup> E. Anderson, *Annual Review of Nuclear Science* (Annual Reviews, Inc., Stanford, 1953), Vol. 2, p. 63.

<sup>3</sup> J. Arnold and H. Al Salih, *Science* **121**, 451 (1955).

<sup>4</sup> L. Marquez and N. Costa, *Nuovo cimento*, Ser. 10, **2**, 1038 (1955).

<sup>5</sup> L. Winsberg, *Geochim. et Cosmochim. Acta* **9**, 183 (1956).

<sup>6</sup> H. Messel, *Progress in Cosmic-Ray Physics*, edited by J. G. Wilson (Interscience Publishers, Inc., New York, 1954), Vol. II, Chap. IV.

<sup>7</sup> E. George and J. Evans, *Proc. Phys. Soc. (London)* **A63**, 1248 (1950).

<sup>8</sup> H. Messel, *Proc. Phys. Soc. (London)* **A64**, 726 (1951).

atmospheric depth, penetrating 90 g/cm<sup>2</sup> of lead, appears to be  $0.171 \pm 0.005$  particles/cm<sup>2</sup> sec sterad.<sup>9</sup> If one uses the quoted mean free path in lead of 230 g/cm<sup>2</sup>, the primary flux at 54°N (average of 52°–56°N) extrapolated to zero thickness of lead is 0.253 particles/cm<sup>2</sup> sec sterad. This value probably includes the nucleons arising from the breakup of the primary alpha particles as they traverse the lead.<sup>10,11</sup>

At a given geomagnetic latitude, the factor by which the relative total nucleon intensity must be multiplied to yield the absolute total intensity is given by<sup>6</sup>

$$B = 0.253(1.07/E_c)^{1.1}. \quad (1)$$

At 54°N geomagnetic latitude the cut-off energy,  $E_c$ , is 1.07 Bev. Figure 1 gives curves of nucleon flux ( $E_{\text{nucleon}} \geq 500$  Mev) plotted against elevation for several different latitudes. The curve for 59° holds for all latitudes greater than this as the low-energy cut-off, 0.5 Bev, corresponds to 59°.

#### NUCLEON FLUX ( $40 \leq E < 500$ MEV)

It is a more difficult problem to get values for the integral and differential energy spectrum for nucleons with energies below 500 Mev with the same accuracy as for nucleons with energies above 500 Mev.<sup>6</sup> By the use of several simplifying approximations, Rossi<sup>12</sup> has derived the following equations to represent the vertical differential energy spectrum of protons and neutrons for nucleon energies above 40 to 50 Mev:

For neutrons,

$$J_n(E, h) = \frac{AL_cL \exp(-h/L) - \exp(-h/L_c)}{(L - L_c)(50 + E)^2}. \quad (2)$$

For protons,

$$J_p(E, h) = \frac{A \exp(-h/L) \left[ \frac{1}{50 + E} - \frac{1}{50 + E_m} \right]}{k(E)}. \quad (3)$$

where  $J_n(E, h)$  and  $J_p(E, h)$  represent the differential neutron and proton fluxes in the vertical direction at atmospheric depth  $h$  and energy  $E$ . The constant  $A$  is determined empirically;  $L$  and  $L_c$  are the absorption and interaction mean free paths of the radiation generating these lower energy nucleons;  $k(E)$  is the specific ionization loss of a proton of energy  $E$ ; and  $E_m$  is the energy that a primary proton must have upon entering the top of the atmosphere such that its energy loss by ionization will bring its energy down to  $E$  when it has reached depth  $h$ .

Equations (2) and (3) have been derived assuming a straight exponential dependence of the flux on the

<sup>9</sup> E. Dymond, *Progress in Cosmic-Ray Physics*, edited by J. G. Wilson, (Interscience Publishers, Inc., New York, 1954), Vol. II, pp. 120–121.

<sup>10</sup> B. Rossi, *High-Energy Particles* (Prentice-Hall, Inc., New York, 1952), pp. 520–522.

<sup>11</sup> G. McClure, *Phys. Rev.* **96**, 1391 (1954).

<sup>12</sup> B. Rossi, *High-Energy Particles* (Prentice-Hall, Inc., New York, 1952), pp. 486–490.

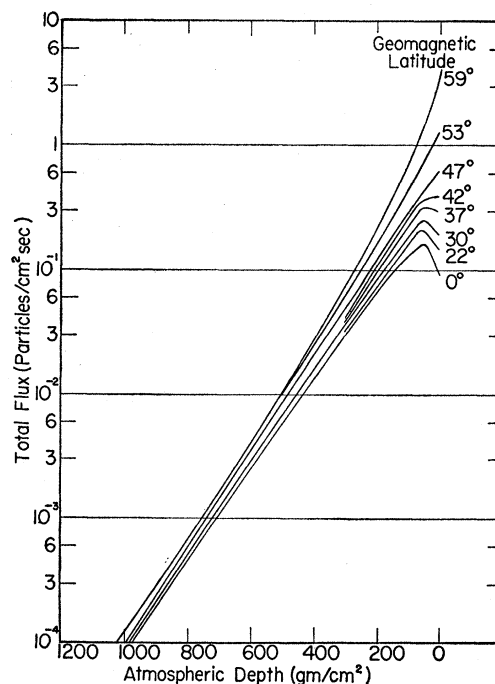


FIG. 1. High-energy nucleon intensity vs atmospheric depth,  $E \geq 500$  Mev.

depth. Since the more accurate theory shows the increasing deviation from exponential dependence of the flux on depth at higher elevations, the errors in Eqs. (2) and (3) will increase as the elevation increases. In this work the exponential dependence has been assumed to hold from sea level to  $h = 250$  g/cm<sup>2</sup> depth. At 250 g/cm<sup>2</sup> depth the errors in Eqs. (2) and (3) are substantial, but are not so large as to invalidate the use of these equations.

The constant  $A$  is determined by first finding the integral energy flux for neutrons in the vertical direction for energies  $\geq 500$  Mev, as derived from integrating Eq. (2). This number, which includes  $A$ , is set equal to the values of the vertical neutron flux for  $E \geq 500$  Mev as given in Fig. 14, of reference 6, multiplied by the factor  $B$  [Eq. (1)]. A value of  $A$  was determined at two depths, 250 and 1000 g/cm<sup>2</sup>, for each curve representing a certain geomagnetic latitude corresponding to the given  $E_c$  ( $E = 500$  Mev). The values of  $A$  at the two depths differed from each other by about 20%. This error includes the deviations from exponential dependence (which are included in the more complete theory presented by Messel<sup>6</sup>). The average value of  $A$  for the two depths was used for each latitude. Values of  $L$  and  $L_c$  were taken as 140 g/cm<sup>2</sup><sup>13</sup> and 75 g/cm<sup>2</sup><sup>8</sup> for determining  $A$ .

In order to obtain the total neutron and proton flux for energies greater than  $E$  and less than 500 Mev and from all directions, Eqs. (2) and (3) must be integrated with respect to  $E$  and  $\theta$ . To do this,  $h$  is replaced

<sup>13</sup> J. Simpson and W. Fagot, *Phys. Rev.* **90**, 1068 (1953).

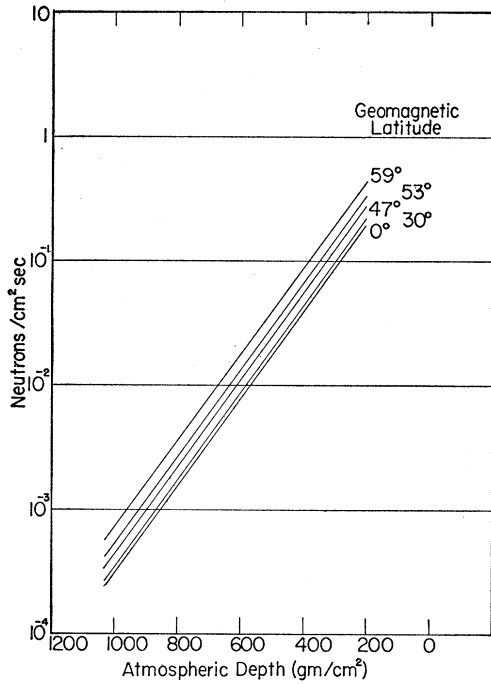


FIG. 2. Neutron flux vs atmospheric depth,  $40 \text{ Mev} \leq E_n < 500 \text{ Mev}$ .

by  $h/\cos\theta$ , the atmospheric depth in the direction  $\theta$ , and the equations are integrated over all directions. Performing this integration for neutrons on Eq. (2), and integrating again with respect to energy, gives the result

$$N(E, h) = \frac{2\pi L_c L A \Gamma}{L - L_c} \left[ \frac{1}{50 + E} - \frac{1}{550} \right] \times \left[ \exp\left(\frac{-h}{L}\right) - \exp\left(\frac{-h}{L_c}\right) + \frac{h}{L} \text{Ei}\left(\frac{-h}{L}\right) - \frac{h}{L_c} \text{Ei}\left(\frac{-h}{L_c}\right) \right]. \quad (4)$$

Here  $N(E, h)$  is the total neutron flux over all angles at vertical depth  $h$ , for neutrons with energy  $\geq E$  Mev. Ei refers to the exponential integral, values of which are tabulated in the literature. Curves of  $N(E, h)$  are given in Fig. 2 for different  $h$  and geomagnetic latitudes, with  $E = 40$  Mev.

In order to obtain the integral proton flux over all directions and between 40 and 500 Mev, Eq. (3) must be integrated over all directions and over the correct energy region. This, however, is difficult, as  $E_m$  is a complex function of the zenith angle. However, if a simplifying approximation is made for  $E_m$ , Eq. (3) can be handled with relative ease. An examination of  $E_m$  and proton range data for air<sup>14</sup> shows that even at  $h = 250 \text{ g/cm}^2$ , the quantity  $1/(50 + E_m)$  is smaller

than  $1/(50 + E)$ . Therefore, an approximation to  $E_m$  should be chosen which fits fairly well for this extreme case of  $h = 250 \text{ g/cm}^2$ . A bad fit at larger depths will not be so important, since then  $1/(50 + E)$  is much larger than  $1/(50 + E_m)$ . Also, any error made by use of this approximation is reduced by a factor of about 6 when the total nucleon flux is determined, since the proton flux described above is approximately  $\frac{1}{6}$  of the total nucleon flux with  $E \geq 40$  Mev. The approximation chosen for  $E_m$  is  $1/(50 + E_m) = 1/(4x)$  as this gives an integrable function. Equation (3) now becomes

$$J_p(E, x) = \frac{A \exp(-x/L)}{k(E)} \left[ \frac{1}{50 + E} - \frac{1}{4x} \right]. \quad (5)$$

To integrate Eq. (5) over all directions,  $x$  the depth at an angle  $\theta$  from the zenith is replaced by  $h/\cos\theta$  and  $2\pi \sin\theta d\theta$  is multiplied in as the differential surface element. The expression is then integrated from 0 to  $\pi/2$ . The final expression for the integral proton spectrum over all directions and with energy  $\geq E$  but less than 500 Mev is

$$P(E, h) = 2\pi A h \left\{ \left[ -\frac{\exp(-h/L)}{8h^2} + \frac{\exp(-h/L)}{8hL} + \frac{1}{8L^2} \text{Ei}\left(\frac{-h}{L}\right) \right] \int_E^{500} \frac{dE}{k(E)} + \left[ \frac{\exp(-h/L)}{h} + \text{Ei}\left(\frac{-h}{L}\right) \right] \times \int_E^{500} \frac{dE}{k(E)(50 + E)} \right\}. \quad (6)$$

The integrals

$$\int_E^{500} \frac{dE}{k(E)} \quad \text{and} \quad \int_E^{500} \frac{dE}{k(E)(50 + E)}$$

were evaluated numerically using the available specific ionization data of air.<sup>14</sup> With a lower limit for  $E$  of 40 Mev, the resulting values for the integrals are  $136 \text{ g/cm}^2$  and  $0.44 \text{ g/cm}^2 \text{ Mev}$ , respectively. Substitution of these values into Eq. (6) along with the (previously calculated) values of  $A$  gives the integral proton flux. Figure 3 gives curves of the integral proton flux over all directions and for  $40 \text{ Mev} \leq E_p < 500 \text{ Mev}$  for different depths and geomagnetic latitudes.

#### NUCLEON FLUX ( $E \geq 40$ MEV)

In order to get the total nucleon flux for  $E_{\text{nucleon}} \geq 40$  Mev, and up to  $250 \text{ g/cm}^2$  atmospheric depth, the values for the flux given in Figs. 1, 2, and 3 for the same altitude and latitude must be added together. The results are plotted in Fig. 4.

A point is also given for the top of the atmosphere for each geomagnetic latitude. These points are taken

<sup>14</sup> J. Smith, Phys. Rev. 71, 32 (1937).

directly from Fig. 1 as the secondary flux is zero at zero depth.

Between the points given at 0 and 250 g/cm<sup>2</sup> atmospheric depth, the nucleon flux was estimated in the following somewhat empirical manner:

Since the star production rate in nuclear emulsions should be proportional to the high-energy nucleon flux ( $E_{\text{nucleon}} \geq 20\text{--}30$  Mev),<sup>15</sup> any experimental star-production data at depths less than 250 g/cm<sup>2</sup> should give the nucleon flux for the region in question. Figure 5 is a curve drawn through Lord's<sup>16</sup> experimental points giving the star-production rate at 52°–56°N geomagnetic latitude as a function of atmospheric depth. This curve is normalized to the total nucleon flux for 53°, at the top of the atmosphere. The point at 250 g/cm<sup>2</sup> depth and 53° on Fig. 4 almost coincides with the normalized star-production-rate curve. This agreement gives some support to the use of the above normalized curve to represent the total high-energy nucleon flux at small depths.

In order to derive total flux curves for the upper 250 g/cm<sup>2</sup> depth for latitudes other than 53°, the above normalized curve is renormalized to the curves in Figs. 1 and 4. This is somewhat complicated by the fact that the average primary energy is higher for lower latitudes resulting in more secondaries per primary. Appropriate arithmetical operations were used to account for this fact. The portions of the curves in Fig. 4 down to 250

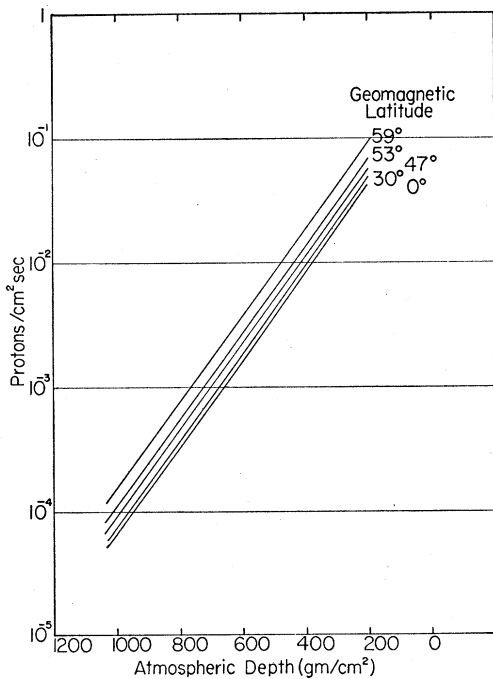


FIG. 3. Proton flux vs atmospheric depth 40 Mev  $\leq E_p < 500$  Mev.

<sup>15</sup> M. Blau *et al.*, Phys. Rev. 91, 949 (1951).  
<sup>16</sup> J. Lord, Phys. Rev. 81, 901 (1951).

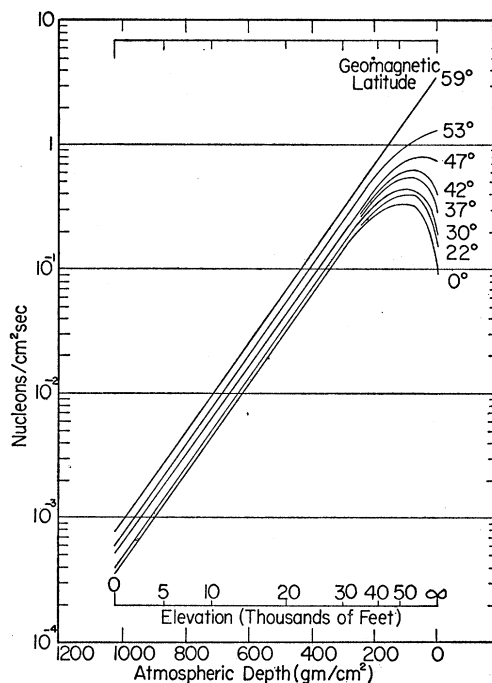


FIG. 4. Total nucleon flux vs atmospheric depth  $E_{\text{nucleon}} \geq 40$  Mev.

g/cm<sup>2</sup> depth give the results of the renormalization for each latitude.

The curves in Fig. 4 would be slightly altered by recent experimental evidence<sup>17,18</sup> indicating that both the primary spectrum and low-energy cutoff may change slightly with time. The spectrum changes will be neglected in view of the approximations appearing in this work. For increases or decreases in the cutoff energy, curves have to be subtracted from or added to those already given in Figs. 1–4 and 8.

#### Be<sup>7</sup> PRODUCTION CROSS SECTION

In order to calculate the amount of Be<sup>7</sup> produced in the atmosphere, the cross section for Be<sup>7</sup> production from air must be known as a function of nucleon energy. The atmosphere will be assumed to consist of nitrogen only, as the excitation function for Be<sup>7</sup> production from oxygen should be similar to that from nitrogen. The maximum error expected from this source is about 5%.<sup>19</sup>

The least endoergic routes for Be<sup>7</sup> production from nitrogen by neutrons and protons are given below with their respective  $Q$  values:

$$1(a): N^{14} + n = Be^7 + Li^8, \quad Q = -25.7 \text{ Mev,}$$

$$2(a): N^{14} + p = Be^7 + 2He^4, \quad Q = -10.4 \text{ Mev.}$$

No data on cross sections for the reactions  $N(p, X)Be^7$

<sup>17</sup> P. Meyer and J. Simpson, Phys. Rev. 99, 1517 (1955).

<sup>18</sup> H. Neher and E. Stern, Phys. Rev. 98, 845 (1955).

<sup>19</sup> P. Benioff and M. Kalkstein (preliminary unpublished results).

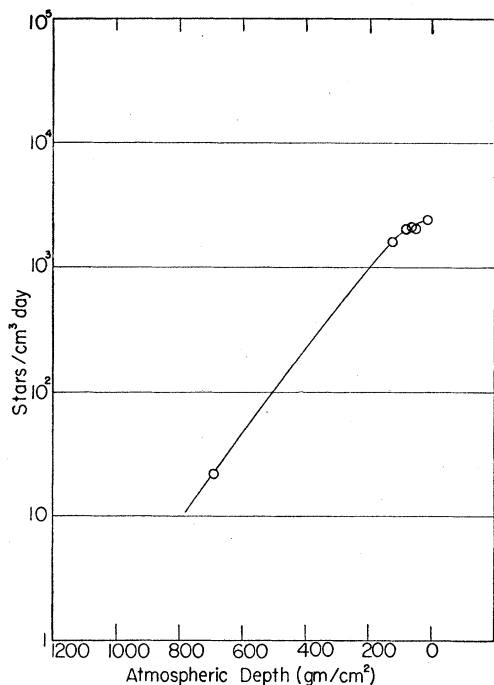


Fig. 5. Lord's star production rate in emulsion at 52°–56°N geomagnetic latitude vs atmospheric depth.

or  $N(n,X)Be^7$  have been found in the literature. However, the excitation function for  $Be^7$  production from carbon by protons of energy up to 5.7 Bev is available<sup>19–21</sup> and is given in Fig. 6.<sup>22,23</sup> Since most of the excitation functions for the light elements have about the same shape,<sup>23–26</sup> the assumption will be made that the shapes of the excitation functions for the reactions  $N^{14}(p,X)Be^7$  and  $N^{14}(n,X)Be^7$  are the same as that of the curve in Fig. 6. It will also be assumed that at Bev energies the absolute values of the  $Be^7$  production cross section for protons is the same as that for neutrons. It can be seen from Fig. 6 that the maximum in the excitation function occurs about 30 Mev above the  $|Q|$  value (26 Mev) for the reaction. This differential of 30 Mev will be taken to hold for  $Be^7$  production from nitrogen by neutrons and protons. Consequently, the proton excitation function for  $N^{14}(p,X)Be^7$  may be approximated by shifting the energy scale on the

<sup>20</sup> J. Dickson and T. Randle, Proc. Phys. Soc. (London) **A64**, 902 (1951).

<sup>21</sup> L. Marquez and I. Perlman, Phys. Rev. **81**, 953 (1951).

<sup>22</sup> The point at 335 Mev<sup>21</sup> on Fig. 6 has been multiplied by 36/41. This has been done because recent careful work<sup>23</sup> has shown that the previous values of the cross section for the monitor reaction,  $C^{12}(p,pn)C^{11}$  were slightly in error. The values for the excitation function for  $Be^7$  produced from carbon at energies  $\leq 160$  Mev<sup>20</sup> may also be in error for the above reason. Since the  $C^{12}(p,pn)C^{11}$  monitor reaction has not been checked at the lower energies, it will be assumed that the values given in reference 20 are correct.

<sup>23</sup> W. Crandall *et al.*, Phys. Rev. **101**, 329 (1956).

<sup>24</sup> N. Hintz and N. Ramsey, Phys. Rev. **88**, 19 (1952).

<sup>25</sup> R. Wolfgang and G. Friedlander, Phys. Rev. **96**, 190 (1954).

<sup>26</sup> G. Friedlander *et al.*, Phys. Rev. **99**, 263 (1955).

$C^{12}(p,X)Be^7$  excitation function curve so that the maximum occurs at 40 Mev (30+10). The  $Q$  value for the reaction  $N^{14}(n,X)Be^7$  is almost the same as that for the reaction  $C^{12}(p,X)Be^7$ , so no shifting of the energy scale is necessary. The excitation functions for neutron and proton production of  $Be^7$  from nitrogen can be obtained by multiplying the above two excitation functions by the experimentally observed cross-section ratio for  $N(p,X)Be^7/C(p,X)Be^7$  at  $E_p=5.7$  Bev,<sup>19</sup> and are given in Fig. 7.

#### ATMOSPHERIC BERYLLIUM-7 PRODUCTION

The total amount of  $Be^7$  produced (per unit time and weight of air) as a function of latitude and altitude,  $D(h)$ , is given by

$$D(h) = C \int_{E_{nth}}^{\infty} \sigma_n(E) J_n(E, h) dE + C \int_{E_{pth}}^{\infty} \sigma_p(E) J_p(E, h) dE, \quad (7)$$

where  $C$  is a constant whose value depends on the units for  $D(h)$ .  $E_{nth}$  and  $E_{pth}$  are the neutron and proton reaction energy thresholds. The quantities  $J_n(E, h)$  and  $J_p(E, h)$  are the differential neutron and proton fluxes respectively at depth  $h$  and energy  $E$ , per unit energy interval. Exclusive of any meson contribution to  $Be^7$  production Eq. (7) holds exactly. For the purposes of this work, several simplifying steps may be taken. The approximate nature of Eqs. (2) and (3) allows the replacement of both integrals in Eqs. (7) by a product of the average production cross section and the total nucleon flux. The average  $Be^7$  production cross section by neutrons can be calculated from

$$\langle \sigma_n(E) \rangle_{Av} = \frac{\int_{40 \text{ Mev}}^{5.7 \text{ Bev}} \sigma_n(E) J_n(E, h) dE}{\int_{40 \text{ Mev}}^{5.7 \text{ Bev}} J_n(E, h) dE}. \quad (8)$$

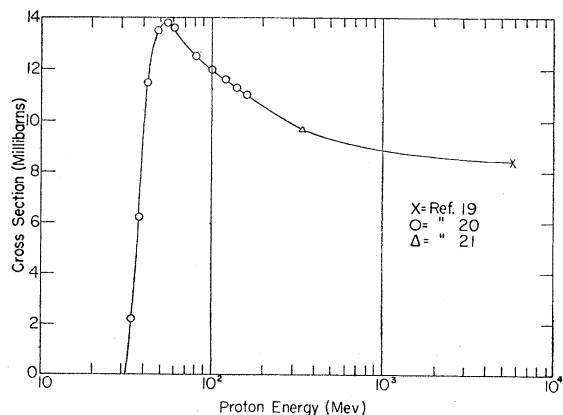


Fig. 6. Excitation function for  $Be^7$  production from carbon.

The expression for  $\langle\sigma_p(E)\rangle_{Av}$  is the same as Eq. (8) with the subscripts  $n$  replaced by  $p$ . For a numerical evaluation of Eq. (8), the curves in Fig. 7 are used for  $\sigma_n(E)$  and  $\sigma_p(E)$ , and Eqs. (2) and (3) are used for  $J_n(E, h)$  and  $J_p(E, h)$ . The change of the limits of integration in Eq. (8) introduces only small errors because of the rapid decrease of Eq. (3) and the curves in Fig. 7 for decreasing low energies and because of the rapid decrease of Eqs. (2) and (3) with increasing high energies.

An examination of Figs. 2 and 3 shows that the neutron-to-proton flux ratio is approximately constant for most latitudes and altitudes. Also  $\langle\sigma_n(E)\rangle_{Av}$  is almost equal to  $\langle\sigma_p(E)\rangle_{Av}$ . Thus Eq. (7) may be simplified to give

$$D(h) = C(\langle\sigma\rangle_{Av})[N(h) + P(h)], \quad (9)$$

where  $\langle\sigma\rangle_{Av}$  is the average of  $\langle\sigma_p(E)\rangle_{Av}$  and  $\langle\sigma_n(E)\rangle_{Av}$  weighted by the neutron-to-proton ratio as given in Figs. 2 and 3.

Substitution of the values of  $[N(h) + P(h)]$  from Fig. 4 and  $\langle\sigma\rangle_{Av} = 12.9$  mb and  $C = 2.59 \times 10^{24}$  atoms  $\text{sec}^{-1} \text{min}^{-1}$  in Eq. (9) gives the number of atoms of  $\text{Be}^7$  produced per minute per gram. Curves of  $D(h)$  as

TABLE I. Neutron and proton flux ratios.

Geomagnetic latitude, $\Phi$	Neutron flux ratio $N(\Phi)/N(O)$		Proton flux ratio $N(\Phi)/N(O)$	
	312 g/cm <sup>2</sup> from Fig. 3	depth (experimental)	680 g/cm <sup>2</sup> from Fig. 3	depth (experimental)
30	1.1	1.7-1.9	1.1	1.5
47	1.4	3.2-3.6	1.4	2.4
53	1.7	3.3-4.3	1.7	2.6

atoms  $\text{Be}^7$  produced per minute per gram of air are given in Fig. 8 for various geomagnetic latitudes as a function of altitude.

COMPARISON WITH EXPERIMENTAL DATA

The main source of uncertainty in this work is the accuracy with which the curves in Fig. 4 represent the true nucleon flux for  $E \geq 40$  Mev. One estimate of accuracy can be obtained by comparing the theoretical and experimental values of the neutron and proton flux ratio at a given altitude for two different latitudes. Table I gives for two atmospheric depths the ratio of the neutron flux at a latitude  $\Phi$  to that at the geomagnetic equator as obtained from Fig. 2 and from experiment.<sup>27</sup> One comparison of experimental work<sup>27</sup> with results of this work for protons is also included.

It is immediately apparent that there is disagreement between the experimental and calculated ratios. A reason for part of the disagreement is that for the experimental data which include neutrons of energy range 1-30 Mev, equilibrium is not reached until an atmospheric depth of  $\approx 500$  g/cm<sup>2</sup>.<sup>27</sup> For the calculated

<sup>27</sup> J. Simpson *et al.*, Phys. Rev. **90**, 934 (1953); J. Simpson, Phys. Rev. **83**, 1175 (1951).

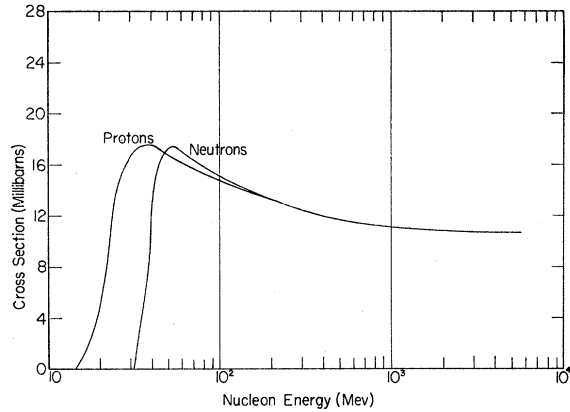


Fig. 7. Excitation function for  $\text{Be}^7$  production from nitrogen.

numbers, which represent neutrons of energy range 40-500 Mev, equilibrium would be reached at a smaller depth and consequently the calculated ratios should be in better agreement with the experimental data at 680 g/cm<sup>2</sup> depth than at 312 g/cm<sup>2</sup>. This is just what Table I indicates. It should also be kept in mind that the accuracy of the curves in Fig. 4 is probably lowest for the region between 250-500 g/cm<sup>2</sup> owing to the exponential dependence used up to 250 g/cm<sup>2</sup> depth. The agreement between the calculated and observed latitude effect is as good as can be expected if allowance is made for the above reasons as well as for the approximations made in the calculations.

The experimentally observed star-production rate is more appropriate for an accuracy determination than

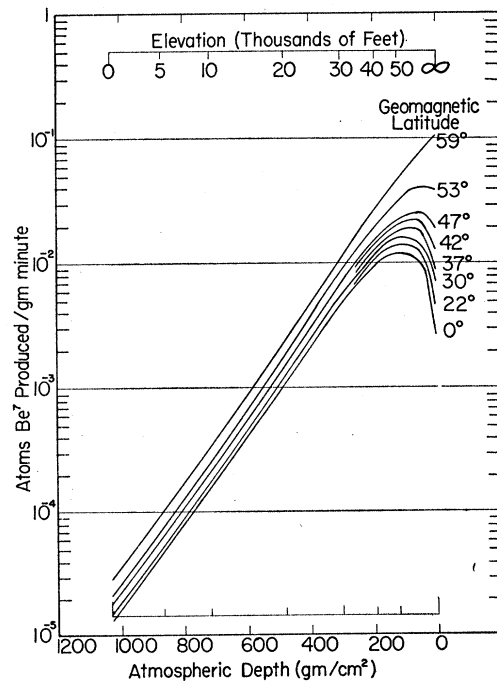


Fig. 8.  $\text{Be}^7$  production rate vs atmospheric depth.

TABLE II. Cosmic-ray star production rate.

Atmospheric depth g/cm <sup>2</sup>	Geomagnetic latitude	Star-production rate in film		Nucleon flux from Fig. 4, particles cm <sup>-2</sup> sec <sup>-1</sup>	Star production cross section mb	Reference
		All stars cm <sup>-3</sup> day <sup>-1</sup>	Stars due to C,N,O nuclei cm <sup>-3</sup> sec <sup>-1</sup>			
1030	45°N	0.6	1.74×10 <sup>-6</sup>	5.1×10 <sup>-4</sup>	132	32
370	45°N	200	5.79×10 <sup>-4</sup>	0.110	204	32
218	45°N	800	2.31×10 <sup>-3</sup>	0.37	242	32
680	54°N	22	6.36×10 <sup>-5</sup>	0.0100	246	16
120	54°N	1610	4.66×10 <sup>-3</sup>	0.91	196	16
81	54°N	2040	5.90×10 <sup>-3</sup>	1.07	213	16
64	54°N	2150	6.22×10 <sup>-3</sup>	1.12	215	16
47	54°N	2030	5.87×10 <sup>-3</sup>	1.19	191	16
15	54°N	2390	6.91×10 <sup>-3</sup>	1.30	206	16
47	28°N	425	1.23×10 <sup>-3</sup>	0.43	110	16
15	28°N	575	1.66×10 <sup>-3</sup>	0.30	214	16
595	1°S	12	3.47×10 <sup>-5</sup>	0.0120	112	37
680	47°N	13.5	3.90×10 <sup>-5</sup>	8.5×10 <sup>-3</sup>	178	34
195	47°N	1125	3.25×10 <sup>-3</sup>	0.47	268	34
680	47°N	16.2	4.68×10 <sup>-5</sup>	8.5×10 <sup>-3</sup>	213	33
1030	54°N	1.46	4.22×10 <sup>-6</sup>	6.1×10 <sup>-4</sup>	267	6
680	43°N	14.2	4.11×10 <sup>-5</sup>	8.2×10 <sup>-4</sup>	194	35
14	55°N	1960	5.67×10 <sup>-3</sup>	1.8	120	36
905	41°N	2.64	7.64×10 <sup>-6</sup>	1.65×10 <sup>-3</sup>	179	31
11	41°N	815	2.36×10 <sup>-3</sup>	0.52	176	31
Average: 194±54 mb						

the latitude effect. The amount of Be<sup>7</sup> produced at any point in the atmosphere should be proportional to the star-production rate at that point with the proportionality constant remaining approximately the same throughout the atmosphere. One reason is that nuclear stars have been observed with neutron energies down to about 20 Mev which is close to the Be<sup>7</sup> production threshold. Another reason is that the star-production cross section in nitrogen<sup>28-30</sup> and the average Be<sup>7</sup> production cross section change slowly with variations in the nucleon energy spectrum.

The star-production rate in film at different latitudes and altitudes as measured by several authors<sup>6,16,31-37</sup> is given in column 3 of Table II. The nuclear star data, used before for the upper 250 g/cm<sup>2</sup> of atmosphere at 52°-56°N,<sup>16</sup> is included in Table II only as a check on the absolute magnitude of the curves given in Fig. 4. It is included in the average given at the bottom of the table, but is excluded from the standard deviations, since it was used to determine the shape of part of the curves in Fig. 4. About 25% of the stars produced in film originate from light elements, C, N, and O, and there are 2.58×10<sup>22</sup> C, N, and O atoms/cm<sup>3</sup> emulsion.<sup>15,16</sup> The star-production rate due to light nuclei is given in column 4. The nucleon flux at the given altitude and latitude obtained from Fig. 4 is given in column 5, and the next column contains the star-pro-

duction cross section for light nuclei calculated from the previous factors.

The average star-production cross section as obtained from Table II is 194±54 mb. The standard deviation, 28%, is quite satisfactory since it also includes the error in the experimental star production rate determinations. A recent series of measurements<sup>31</sup> indicates that the standard deviation from this latter source of error is at least 18%. The value of 28% should be accepted somewhat tentatively since the experimental data given in Table II are somewhat sketchy in terms of latitude coverage of the atmosphere.

The star-production cross section for nitrogen is approximately known at several different energies<sup>28-30</sup> and varies from about 170 mb at 45-Mev proton energy to 200 mb at 950-Mev proton energy. The star-production rates given<sup>16,31-37</sup> in Table II are for stars with more than two prongs. All the stars observed at 950 Mev,<sup>30</sup> and 84% of the stars at 45 Mev<sup>29</sup> have more than two prongs. Thus, the average of 194±54 mb from Table II can be compared directly with the range 170-200 mb from accelerator experiments, and the observed agreement is excellent.

From the above considerations the conclusion can be drawn that, despite the approximate nature of the data given in Figs. 2 and 3, the total nucleon flux given in Fig. 4 agrees reasonably well with the available experimental data. When the errors in the Be<sup>7</sup> production cross section are also included, the over-all error limits on the Be<sup>7</sup>-production rate as given in Fig. 8 are probably no greater than ±50%.

#### APPLICATION OF Be<sup>7</sup> PRODUCTION RATE TO THE ATMOSPHERE IN MOTION

The previous production rate of Be<sup>7</sup> as derived, is equal to the disintegration rate only for a stationary

<sup>28</sup> P. E. Hodgson, *Phil. Mag.* **44**, 1113 (1953).

<sup>29</sup> P. E. Hodgson, *Phil. Mag.* **45**, 190 (1954).

<sup>30</sup> W. Lock *et al.*, *Proc. Roy. Soc. (London)* **A230**, 215 (1955).

<sup>31</sup> H. Yagoda, *Can. J. Phys.* **34**, 122 (1956).

<sup>32</sup> H. Forster, *Phys. Rev.* **78**, 247 (1950).

<sup>33</sup> J. Harding, *Phil. Mag.* **42**, 651 (1951).

<sup>34</sup> N. Page, *Proc. Phys. Soc. (London)* **A63**, 250 (1950).

<sup>35</sup> G. Bernardini *et al.*, *Phys. Rev.* **79**, 952 (1950).

<sup>36</sup> M. Addario and S. Tamburino, *Phys. Rev.* **76**, 983 (1946).

<sup>37</sup> G. Beets *et al.*, *Compt. rend.* **229**, 1227 (1949).

atmosphere with no washout. However, the earth's atmosphere is constantly moving and being cleaned. A detailed account of the various processes and how they affect the local  $\text{Be}^7$  concentration is exceedingly complex. However, a general  $\text{Be}^7$  inventory of the atmosphere which includes the rain-water data and the theoretical production rate given in Fig. 8 allows the calculation of certain atmospheric parameters as functions of others. Consider, for example, the  $\text{Be}^7$  mean removal times. In this paper, the mean removal time is defined as follows: If, in a given volume of air, the cosmic-ray production and radioactive decay of  $\text{Be}^7$  were to cease, the mean removal time is the time it takes for the initial  $\text{Be}^7$  concentration to decrease to  $1/e$  of its original value.

The  $\text{Be}^7$  inventory in the troposphere can be set up as follows: For the troposphere, which is the layer of air extending from sea level to the base of the stratosphere, taken here to be at 35 000-ft elevation,<sup>38</sup> the following equation should hold:

$$dN_T/dt = P_T + R_S - \lambda N_T - R_T. \quad (10)$$

For the stratosphere, which here includes all the atmosphere above the troposphere, the expression similar to Eq. (10) is

$$dN_S/dt = P_S - R_S - \lambda N_S. \quad (11)$$

$dN/dt$  is the time rate of change of  $\text{Be}^7$  concentration,  $N$  is the  $\text{Be}^7$  concentration in atoms/cm<sup>2</sup>,  $P$  and  $R$  are the production and removal rates of  $\text{Be}^7$  in atoms/cm<sup>2</sup> min, and  $\lambda$  is the  $\text{Be}^7$  radioactive decay constant. The subscripts  $S$  and  $T$  refer to the stratosphere and troposphere respectively. Since rain clouds rarely occur in the stratosphere, the main process, besides decay, by which  $\text{Be}^7$  can be removed from the stratosphere is by mixing with the troposphere. The stratosphere has a higher concentration of  $\text{Be}^7$  than the troposphere, so any mixing would decrease the stratosphere and increase the troposphere concentration. This is expressed by the plus and minus signs before  $R_S$  in Eqs. (10) and (11) respectively. Recently it has been shown that about four times as much radioactive dust is removed by rainfall as by direct settling.<sup>39</sup> Since  $\text{Be}^7$  probably exists in very small particles, direct settling probably removes even less than 20% and can be neglected here.  $R_T$  can then be set equal to the rainfall removal rate of  $\text{Be}^7$  from the troposphere.

In general the rates  $dN_S/dt$  and  $dN_T/dt$  will not be equal to zero. One reason is that the atmospheric  $\text{Be}^7$  concentration at ground level has been shown to change with the seasons.<sup>40</sup> Other contributing factors are changes in the low-energy cutoff and slow changes in the primary proton spectrum.<sup>17,18</sup> However, Eqs. (10) and

(11) will be limited in this work to the use and derivation of values of the parameters averaged over one year. For this reason all cyclical annual changes can be ignored. Any noncyclical changes are small in comparison to the approximations used previously. Consequently  $dN_S/dt$  and  $dN_T/dt$  may be set equal to zero.

The removal rate of  $\text{Be}^7$  from the troposphere,  $R_T$ , may be set equal to

$$R_T = \lambda_T N_T, \quad (12)$$

where  $\lambda_T = 1/t_T$  is the reciprocal mean removal time from the troposphere. Equation (12) should be correct if precipitation is considered as a sweeping-out process, since the amount swept out should be proportional to the troposphere concentration. The same relationship will be used for the removal rate from the stratosphere, although the removal processes are not as well known. As in Eq. (12) an effective mean removal rate for the stratosphere,  $R_S$ , will be then given by

$$R_S = N_S/t_S. \quad (13)$$

$P_S$  and  $P_T$  are found by graphically integrating the curves in Fig. 8 over a geomagnetic hemisphere of the earth's surface (the two hemispheres should be equal). The curve in Fig. 8 for 59° is used for all latitudes between 59° and the geomagnetic north pole. The use of 35 000 ft as the tropopause elevation gives  $P_T = 1.3$  atoms/cm<sup>2</sup> min and  $P_S = 5.0$  atoms/cm<sup>2</sup> min.

The average annual removal rate of  $\text{Be}^7$  is calculated from the experimental  $\text{Be}^7$  concentration in rainwater and the total annual rainfall for a given location. The average annual removal rates for Chicago, Illinois<sup>3</sup> and Bombay, India<sup>41</sup> turn out to be 0.94 atom/cm<sup>2</sup> min and 0.84 atom/cm<sup>2</sup> min respectively. The extrapolation will be made here that the average of these two values, 0.89 atom/cm<sup>2</sup> min, represents the world-wide average annual removal rate. Some support is given this extrapolation by the fact that the above two rates are so similar for such dissimilar geographies. Also there is recent evidence that the precipitation rates of lingering airborne nuclear test debris are relatively uniform over the earth's surface.<sup>42</sup>

Substitution of Eq. (13) into Eqs. (11) and (10) and the setting of  $dN_S/dt$  and  $dN_T/dt$  equal to zero gives, along with Eq. (12), three equations with four unknowns. The solution of  $t_S$  in terms of  $t_T$  yields the equation

$$t_S = \left( \frac{P_S}{R_T t_T \lambda} - 1 \right) \frac{1}{\lambda}. \quad (14)$$

The  $\text{Be}^7$  half-life is taken as 53.0 days.<sup>43</sup> A curve for  $t_S$  versus  $t_T$  calculated from Eq. (14) is given in Fig. 9. Since the elevation of the base of the stratosphere varies from about 59 000 ft at the equator to about

<sup>38</sup> National Advisory Committee for Aeronautics, Standard Atmosphere Tables and Data, Report No. 218, W. Diehl, October, 1925, reprint, 1948.

<sup>39</sup> N. G. Stewart *et al.*, Atomic Energy Research Establishment Report, Harwell A.E.R.E. HP/R, 1701, June, 1955 (unpublished).

<sup>40</sup> A. Cruikshank *et al.*, Can. J. Chem. 34, 214 (1956).

<sup>41</sup> P. Goel *et al.*, Nuclear Phys. 1, 196 (1956).

<sup>42</sup> W. F. Libby, Science 123, 657 (1956).

<sup>43</sup> J. Hollander *et al.*, Table of Isotopes, University of California Radiation Laboratory Report UCRL-1928, 1952 (unpublished).



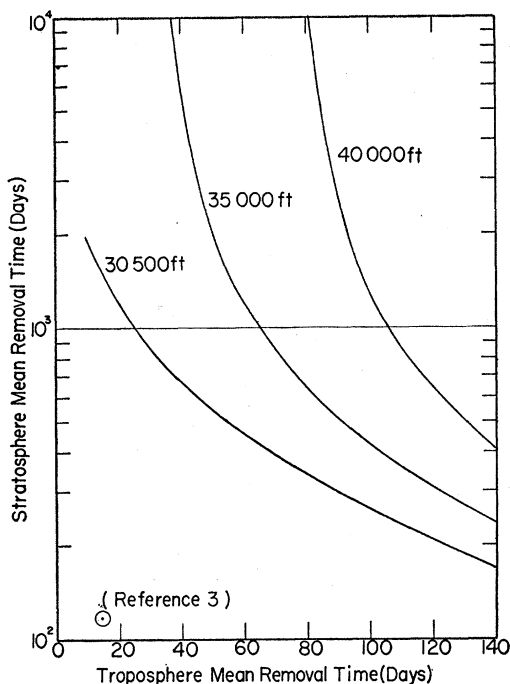


Fig. 9. Stratosphere vs troposphere mean removal times for various tropopause elevations.

22 000 ft at the poles,<sup>44</sup> 35 000 ft may not be a good average tropopause elevation. Consequently, Eq. (14) was solved for two other assumed average tropopause elevations: 30 500 ft (300 g/cm<sup>2</sup>) and 40 000 ft (192 g/cm<sup>2</sup>), and these curves are also presented in Fig. 9.

These curves in Fig. 9 are based on many approximations and extrapolations and consequently should be taken to give only the roughest estimation of the two mean removal times. In spite of these approximations, it is felt that the circled point lies outside the error limits of the curves. This point represents the stratosphere and troposphere mean removal times estimated by Arnold and Al Salih.<sup>3</sup> There are several ways to lower the curves to include the circled point within the error limits. These ways consist of decreasing the geomagnetic cut-off latitude, a lowering the theoretical production rate by 50%, or doubling the mean removal rate by precipitation. Any one of these changes would lower the curves sufficiently. However, the change in the cutoff latitude necessary to produce agreement is quite extreme.<sup>17</sup> Also a 50% decrease in the theoretical production rate would destroy the good agreement between the star production cross section in air derived from the flux curves and that derived from accelerator experiments. It is quite possible, though, that the average Be<sup>7</sup> removal rate is greater than the

<sup>44</sup> G. F. Taylor, *Elementary Meteorology* (Prentice-Hall, Inc., New York, 1954), pp. 68-69.

value used here. The decision as to what the correct value for  $R_T$  is will have to await more experimental data from different parts of the earth.

Upon consideration of the above possible changes and errors in the various parameters making up the curves in Fig. 9, it seems to the author that the best way to resolve the discrepancy is to assume that the annual average removal rate obtained from the rain-water data is approximately correct and that the error lies in the estimated mean removal times of Be<sup>7</sup> from the stratosphere and troposphere. An increase in these times will not only raise the circled point in Fig. 9 but will raise the previously estimated<sup>3</sup> 2.1 atoms/cm<sup>2</sup> min average total production rate of Be<sup>7</sup> closer to the 6.3 atoms/cm<sup>2</sup> min obtained by integrating the curves in Fig. 8. In fact, recent work reported by Libby<sup>42</sup> indicates that the mean removal time may be as large as a few weeks for the troposphere and ten years for the stratosphere. Stewart *et al.*<sup>39</sup> give a troposphere mean removal time of 32 days and indicate a very long stratosphere mean removal time. These more recent estimates of the mean removal times appear to be more in agreement with the work presented in this paper than are the earlier ones.

Perhaps the easiest way to determine the troposphere mean removal time would be to measure experimentally the average troposphere concentration of Be<sup>7</sup>. With this result and the experimental value of  $R_T$ , Eq. (12) allows the direct calculation of a troposphere mean removal time.

The curves shown in Figs. 4, 8, and 9, and Eqs. (12) and (14) show the results of the theoretical calculations and how they may be applied to obtain parameters of atmospheric motion. It is hoped that a more exact theory for the intensity and energy of nucleons produced in the atmosphere as a function of depth for  $E_{\text{nucleon}} < 500$  Mev will appear soon, as the data appearing in Figs. 4 and 8 can then be made more accurate. This, coupled with additional rain-water data for different areas on the earth, would allow a more accurate and detailed use of Eqs. (10)-(14).

*Note added in proof.*—The author's attention has been called to the fact that B. Peters [Proc. Indian Acad. Sci. 4, 67 (1955)] has calculated the atmospheric Be<sup>10</sup> production rate by cosmic rays. His result of 3-6 atoms Be<sup>10</sup> produced/cm<sup>2</sup> min agrees satisfactorily with the Be<sup>7</sup> production rate of 6.3 atoms/cm<sup>2</sup> min calculated in this report provided the Be<sup>10</sup> and Be<sup>7</sup> production cross sections are comparable.

#### ACKNOWLEDGMENTS

The author is grateful to Tracerlab, Western Division, for the time and support made available for this report. The author also wishes to thank H. E. Menker of Tracerlab for the continued advice and support given during the preparation of this report.